Elastic electron scattering and vibrational excitation of isoxazole molecules in the energy range from 2 to 20 eV

Ireneusz Linert and Mariusz Zubek*

Department of Physics of Electronic Phenomena, Gdańsk University of Technology, 80-233 Gdańsk, Poland
(Received 15 June 2012; published 14 August 2012)

Differential cross sections for elastic electron scattering and the excitation of the C-H vibrational modes of isoxazole molecules were measured in the energy range from 2 to 20 eV and over the scattering angle range from 10° to 180°. The cross sections at the scattering angles of and above 90° were accessible with the use of a magnetic angle changer. The differential cross sections were integrated to yield integral and momentum transfer cross sections. The negative ion resonances in the elastic scattering at 2.7 eV and in the vibrational excitation of isoxazole at 5.5 and 10 eV were observed. The present cross sections for elastic scattering are compared with the corresponding results in furan.

I. INTRODUCTION

Investigations of electron interactions with the hydrocarbon heterocyclic molecules, which could be regarded as simple prototypes of the biological compounds, are essential for building our knowledge of the electron induced processes in the polynucleotide strands of DNA. The low-energy (<20 eV) electrons produced in biological tissue by incident ionizing radiation as secondary particles are known to contribute to radiation damage in DNA [1,2]. The effects of radiation on biological tissue are studied experimentally but often also by modeling the electron tracks in the tissue-equivalent materials [3]. For an adequate description the modeling requires, as input data, reliable absolute cross sections for electron interactions with molecules of the tissue-equivalent media such as water and hydrocarbon prototypes of the DNA fragments. Analogous model simulations, which are important in radiotherapy, have been performed for the x-ray microbeam [4] and fast carbon ion beams [5] irradiation techniques.

From the electron-scattering point of view, the experimental studies of electron collisions with heavy heterocyclic molecules in the gas phase are stimulating to develop satisfactory theoretical models for the accurate description of the correlation-polarization interactions and their ramifications on the energy and angular behavior of the scattering cross sections. The recent studies of the differential cross sections (DCSs) in the heavy rare-gas atoms [6] indicated that the DCSs for forward and backward scattering largely depend on the polarizabilities of the atomic targets.

Isoxazole, C_3H_3NO, is a five-membered heterocyclic molecule, which may be derived from furan, C_4H_4O, by replacing a CH group with a nitrogen atom at position (2) in the molecular ring (Fig. 1). It is isoelectronic to furan; therefore both molecules are expected to have similar systems of the excited electronic states. They have, in the ground states, three occupied valence, π_1, π_2, and π_3, and two virtual, π_4^* and π_5^*, molecular orbitals. Furthermore, the molecular geometries, bond distances, and bond angles of furan and isoxazole are predicted in the second-order Møller-Plesset (MP2) and Becke three-parameter Lee-Yang-Parr (B3LYP) calculations to be

similar to within 3%–4% [7]. The isoxazole and furan are planar molecules belonging to the C_s and C_{2v} symmetry point groups, respectively. In the recent studies related to the effects of ionization radiation on biological media, both molecules are regarded as simple prototypes of the components of the backbone and nucleic acids of DNA. Isoxazole and furan have found vital applications in many pharmaceutical products [8]. Despite the similarities, the molecules differ quite substantially with respect to their dipole moments, which are 2.95 ± 0.04 D and 0.66 ± 0.01 D in isoxazole and furan, respectively [9]. However, there is less variance in their polarizabilities, which are 6.61 and 7.27 Å^3, respectively [10]. Finally, it is expected that the comparison of the electron-scattering measurements in both heterocyclic molecules will provide a wider perspective for understanding of the role of the dipole moments and polarization in the electron scattering.

In the present work the DCSs for elastic electron scattering and the vibrational excitation of isoxazole molecules were measured in the energy range from 2 to 20 eV and over a scattering angle range from 10° to 180°. The DCSs for elastic electron scattering in isoxazole are compared with that of furan to display similarities and differences in the electron interaction mechanisms. The previous electron impact investigations of isoxazole are rather scarce. Walker *et al.* [11] measured the near-threshold electron-energy-loss spectra and the total negative ion dissociative electron attachment spectra in the electron-energy region up to 10 eV. They also presented a high-resolution electron-energy-loss spectrum obtained at an electron incident energy of 100 eV and a scattering angle near 0°. The electron transmission spectroscopy of the temporary anion states in isoxazole was carried out by Modelli and Burrow [7] in the low electron-energy region 0.5–4.7 eV. Very recently, Możejko *et al.* [12] measured the total electron-scattering cross section over the energy range 1–400 eV. The electron impact fragmentation studies were performed by Linert *et al.* [13], while the decomposition processes of the molecular ions of isoxazole produced by the electron impact were studied by Bouchoux and Hoppiliard [14]. To our best knowledge, there are no published results of the theoretical studies on electron scattering in isoxazole.

In furan, the elastic DCSs were obtained recently by Khakoo *et al.* [15] at the incident electron energies between
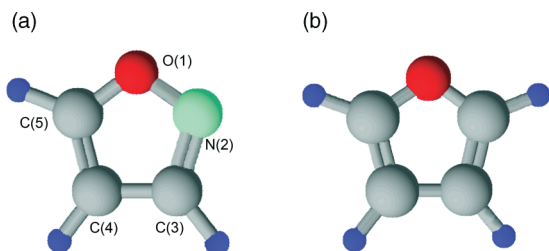
---
*mazub@mif.pg.gda.pl

FIG. 1. (Color online) Schematic diagrams of (a) isoxazole (C_3H_3NO) and (b) furan (C_4H_4O) molecules. Color code: the carbon atom is grey, oxygen atom red, nitrogen atom blue, hydrogen atom dark blue.

1 and 50 eV. The elastic DCSs were also calculated by those authors employing the Schwinger multichannel method with pseudopotentials in the static-exchange (SE) and static-exchange-polarization (SEP) approximations. The vibrational excitation of furan was investigated earlier by Motte-Tollet *et al*. [16] and very recently by Hargreaves *et al*. [17], who determined the DCSs for the excitation of a number of the resolved vibrational modes. The temporary anion states in furan were detected by Modelli and Burrow [7] in their electron transmission studies (0.5–4.7 eV energy range). Finally, the total cross section in furan was measured by Szmytkowski *et al*. [18] in the 0.6–400 eV range.

II. EXPERIMENT

The crossed electron-gas beams spectrometer used in the present measurements was described in detail previously [19]. Briefly, it consists of a source of the selected electron beam, a rotatable scattered-electron analyzer, a source of the gas beam, and a magnetic angle changer at the interaction region.

The electron beam source employs a cylindrical triple-electrode electron gun, a double-hemispherical energy selector, and a triple-electrode output cylindrical lens. The scattered electron analyzer in its design is almost identical to the incident electron beam source, except that the electron gun is replaced by the detector section incorporating the channel electron multiplier. The gas beam is produced by a stainless steel capillary with an inner diameter of 0.6 mm. The analyzer can be rotated around the target beam axis over the angular range from $-90°$ to $90°$ with respect to the direction of the incident electron beam. The electrons scattered at the angles from $90°$ to $180°$ are detected with the use of the magnetic angle changer. The angle changer produces a static, localized magnetic field that is perpendicular to the scattering plane [20]. It deflects the incident electron beam passing through the interaction region, and so all the scattered electrons by the same angle, therefore enabling detection of the electrons scattered at all high scattering angles up to $180°$.

The scattering angle scale was calibrated with an uncertainty of $\pm 2.0°$ against the position of a minimum at $117.5°$ at 10 eV in the elastic electron scattering in argon [21]. The angular resolution of the spectrometer is estimated from the electron optics computations to be less than $5°$. The incident electron energy was calibrated against the position of the $^2P_{3/2}$ negative ion resonance in argon at

11.103 eV [22] with an uncertainty of ± 30 meV. The energy resolution of the spectrometer was 50 meV in the energy-loss mode.

The absolute values of the DCSs for elastic electron scattering from isoxazole were obtained using the relative flow technique [23] with helium as a reference gas. The ratios of scattered electron intensities in isoxazole to those in helium were recorded for fixed incident electron energies at the scattering angles in the range from $10°$ to $180°$ at $10°$ steps. The relative flow rates in isoxazole and helium were determined by the measurements of the increase of pressure in the section of the gas line, which was cut off from the beam forming the capillary. The pressure was monitored with a MKS Baratron capacitance manometer. The absolute DCSs in isoxazole were obtained using the accurate helium theoretical cross sections of Nesbet [24] in the energy range 5–18 eV and that of Saha [25] at 20 eV. The ratio of the driving pressures of isoxazole to that of helium at the entrance to the capillary was maintained at around 0.12, to meet the condition of equal mean-free path lengths in both gases. The driving pressure of isoxazole behind the capillary was below 0.1 mbar. The pressure ratio was estimated taking the molecular diameter of isoxazole to be equal to 6.52 Å, that of thiazole (C_3H_3SN) [26]. It was found, in agreement with the recent observation in tetrahydrofuran [27], that a small deviation of the pressure ratio (to within 5%) from the estimated value produced changes in the measured cross sections, which were much lower than the experimental uncertainties. The elastic-scattering intensities in both gases were corrected for the background scattering, which was determined by flowing the target gas directly to the vacuum chamber and bypassing the gas beam capillary. To obtain stability of the spectrometer operation, a mixture of both gases, isoxazole and helium, was always present in the vacuum chamber; that is, one gas was introduced into the interaction region through the capillary and the other was led directly to the vacuum chamber.

In the studies of vibrational excitation of isoxazole, the energy-loss spectra were recorded for constant incident electron energies at scattering angles in the range from $20°$ to $180°$. The DCSs were obtained for the excitation of the C-H stretch modes ν_1, ν_2, whose energy-loss peaks were clearly seen in the measured spectra. The absolute vibrational DCSs were derived from the intensity ratios of the C-H excitation to the elastic scattering and the measured elastic DCSs. The scattering intensities were corrected for the background contributions. For the scattering angles at and above $90°$, the energy-loss spectra were recorded at a fixed position of the electron analyzer employing the magnetic angle changer. This introduced additional uncertainty into the angular scale of the C-H vibrational excitation of $2°$ at 5 eV and less than $1°$ at higher energies. No corrections for the energy dependence of the transmission of the electron analyzer was introduced, as it was found previously that the analyzer transmission, over the energy-loss range of 0.4 eV, at the present incident electron energies varies by less than 2%.

Isoxazole purchased from Sigma-Aldrich with a declared purity of 99% was degassed several times under vacuum to remove any gaseous impurities. Isoxazole is a liquid at room temperature with a vapor pressure sufficient to obtain vapor flow from a stainless steel container, via a gas line to the
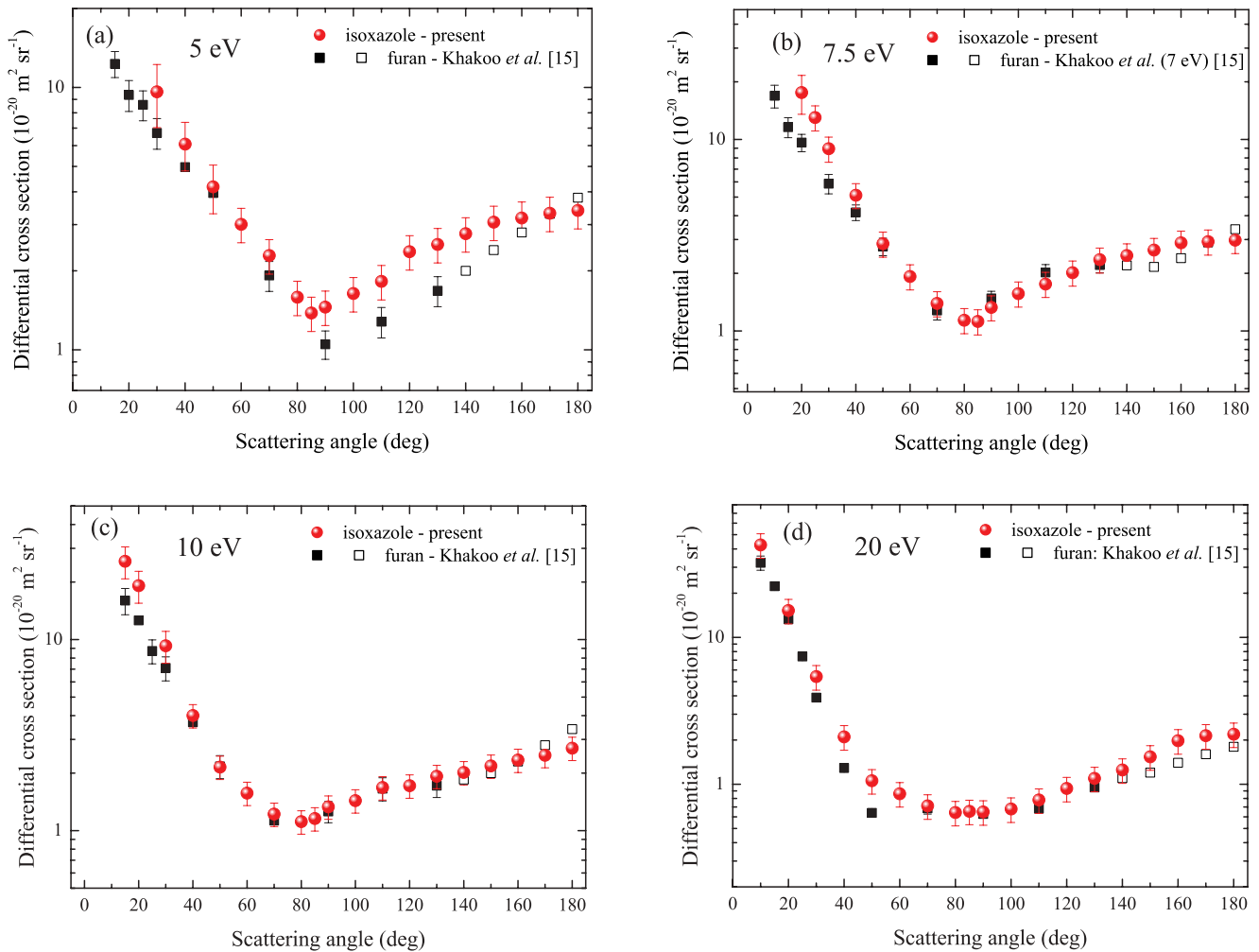
FIG. 2. (Color online) Differential cross sections for electron elastic scattering in isoxazole measured at the energy of (a) 5 eV, (b) 7.5 eV, (c) 10 eV, and (d) 20 eV; full circles show present results. In the figures are also shown differential cross sections measured and extrapolated into the 140°–180° range in furan by Khakoo et al. [15].

scattering region. The gas line was heated to a temperature around 65 °C, the temperature of the spectrometer including the capillary. We have found it essential to maintain the same temperature for the gas line and the capillary. A temperature difference would produce a difference between the flow rates in the section of the gas line where it is measured and at the outlet of the capillary.

The statistical uncertainties in the measured elastic DCSs were determined at each electron energy and scattering angle from series of measurements, typically ten values, and taken to be equal to triple standard deviation (3σ rule). The overall errors include further uncertainties in the helium cross sections of Nesbet [24] and Saha [25], which were taken to be 2% and 2.5%, respectively. The overall uncertainties in the DCSs at 5 eV are 15% but are 27% at 30°, and 21% at 40° and 50°. At 7.5 eV the overall uncertainty is 15% apart from 20°, where it is 23%, while at 10 eV it is 14% but 19% in the 15°–30° range. The uncertainty in the DCSs at 20 eV is 19% in the whole angular range. The uncertainties in the vibrational DCSs include further the uncertainties in the determination of the inelastic to elastic intensity ratios, which are 10%–12% in

the 30°–180° angular range and 20%–22% below that range. The final uncertainties of the vibrational DCSs are obtained by summing in quadrature the uncertainties in the elastic DCSs and that in the intensity ratios and are listed together with the cross section values.

III. RESULTS AND DISCUSSION

A. Elastic electron scattering

1. Differential cross sections

The absolute DCSs measured in isoxazole at electron incident energies of 5, 7.5, 10, and 20 eV are shown in Figs. 2(a)–2(d) and their numerical values are listed in Table I. In Fig. 2, the present cross sections are compared with those measured in furan [15].

The DCS obtained in isoxazole at 5 eV [Fig. 2(a)] shows a minimum at a scattering angle of 85° and below minimum rises steeply with decreasing scattering angle. It is higher than that of furan in general, in the studied angular range; however, it becomes comparable to the extrapolated values

TABLE I. Differential cross sections, in units of 10^{-20} m^2 sr^{-1}, for elastic electron scattering in isoxazole at the incident energies of 5, 7.5, 10, and 20 eV.

Scattering angle	Energy (eV)			
(degrees)	5	7.5	10	20
10	–	–	–	42.7
15	–	–	25.7	–
20	–	17.6	19.1	15.2
25	–	13.0	–	–
30	9.63	8.94	9.28	5.40
40	6.08	5.11	4.00	2.10
50	4.18	2.85	2.15	1.06
60	3.01	1.93	1.57	0.863
70	2.29	1.39	1.22	0.712
80	1.59	1.14	1.11	0.642
85	1.38	1.12	1.16	0.654
90	1.46	1.33	1.33	0.648
100	1.64	1.57	1.43	0.678
110	1.82	1.76	1.68	0.781
120	2.37	2.02	1.72	0.936
130	2.52	2.36	1.93	1.10
140	2.77	2.48	2.02	1.25
150	3.06	2.65	2.18	1.54
160	3.18	2.89	2.34	1.98
170	3.32	2.93	2.48	2.14
180	3.40	2.98	2.70	2.19

of the DCS of furan [15] near 170°. The steep increase of the DCSs in the forward scattering in both molecules results from the dominating long-range dipole interaction. The steeper rise below 60° of the DCS in isoxazole compared to that in furan may be explained by scattering from a higher (4.5 times) dipole moment. Although the polarization interaction may also contribute to the forward scattering [6], it should be comparable in isoxazole and furan as deduced from their polarizabilities, which differ only by 10%. Above 85° the DCS of isoxazole exceeds that of furan presumably as an effect of the contribution of scattering via a shape resonance seen in the vibrational excitation (see below). At 7.5 eV [Fig. 2(b)] and 10 eV [Fig. 2(c)], the present DCSs coincide with those obtained in furan [15] in the 60°–180° angular range, including the extrapolated values of the 140°–180° region. Note that the furan DCSs are measured at 7 eV. Below 60°, the isoxazole DCSs clearly rise faster with the decreasing scattering angle than those of furan. At 20 eV [Fig. 2(d)], the DCS in isoxazole shows a shallow minimum around 85°, more flat than at the lower energies. Differences between DCSs of isoxazole and furan [15] at this energy are noticeable around 50°, where the furan DCS displays a lower value and in the 150°–180° range. Here the extrapolated DCS in furan is lower than that measured in isoxazole.

The energy dependence of the DCS of isoxazole obtained in the 2–20 eV energy range at a scattering angle of 85° is reported in Fig. 3, where it is compared with the DCS of furan measured at a scattering angle of 90° [15]. The isoxazole DCS decreases sharply in the energy range 3–6 eV from a peak near 2.7 eV. Above 6 eV, it further decreases in the whole energy range up to 20 eV (however, less steeply) and
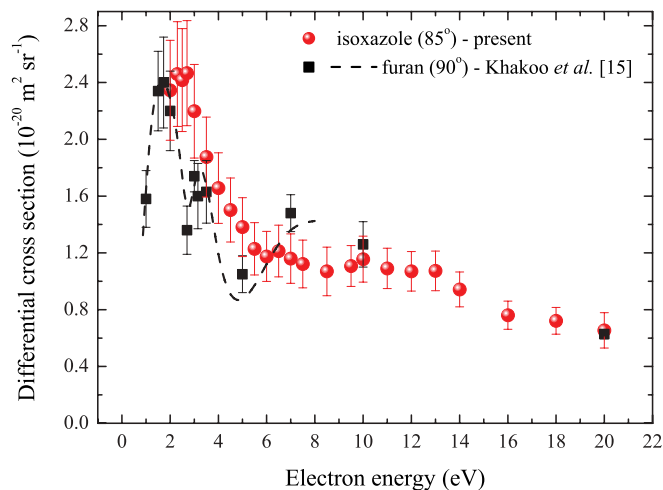

FIG. 3. (Color online) Differential cross section for electron elastic scattering in isoxazole measured at a scattering angle of 85°; full circles show present results. In the figure are also shown results obtained in furan at a scattering angle of 90° by Khakoo *et al.* [15].

in the 9–14 eV range it shows a broad although flat structure. The 2.7-eV peak is produced by scattering via negative ion shape resonance, which we assign to a π^* (π_5^*) resonance, seen previously in the electron transmission measurements at 2.77 eV [7] and in the total cross section near 2.7 eV [12]. The π_5^* resonance at 2.7 eV in isoxazole corresponds to that seen at 3.10 eV in the elastic DCS in furan [15] (see Fig. 3), which was ascribed to the A_2 symmetry [7]. Below 2 eV, the lower limit of the present studies, the transmission measurements carried out in isoxazole [7] revealed a π^* (π_4^*) shape resonance at 1.09 eV, a counterpart of that observed in the elastic scattering in furan at 1.65 eV [15] (Fig. 3), which has the B_1 symmetry [7]. In the 6–9 eV range the isoxazole DCS shows a decrease, while the DCS of furan displays a broad maximum around 8.8 eV, which is well seen in a finer scan of the scattered electron signal as a function of energy [15], shown by a dashed line in Fig. 3. It is worth noting that the theoretical calculations of the integral cross section in furan [28] carried out in the SEP approximation predicted a broad shape resonance in the B_2 symmetry located around 9 eV. The flat structure recorded in the 9–14 eV region in the DCS of isoxazole (Fig. 3) is also seen in the measured total cross section [12].

2. Integral and momentum transfer cross sections

The elastic integral and momentum transfer cross sections were obtained at 5, 7.5, 10, and 20 eV by extrapolating the DCSs down to 0° scattering angle and integrating the DCSs over the complete 0°–180° angular range. To our best knowledge, there are no calculations of the electron elastic scattering from isoxazole that could be used as a guide in the extrapolation. The present DCSs were extended down to 0° by assuming the exponential increase of the cross sections with the decreasing scattering angle. This adopted angular dependence was examined using the DCSs of furan [15] and was found to yield the integral cross sections within 5% of those obtained in Ref. [15], which employed the calculated DCSs in the extrapolation. The integral and momentum
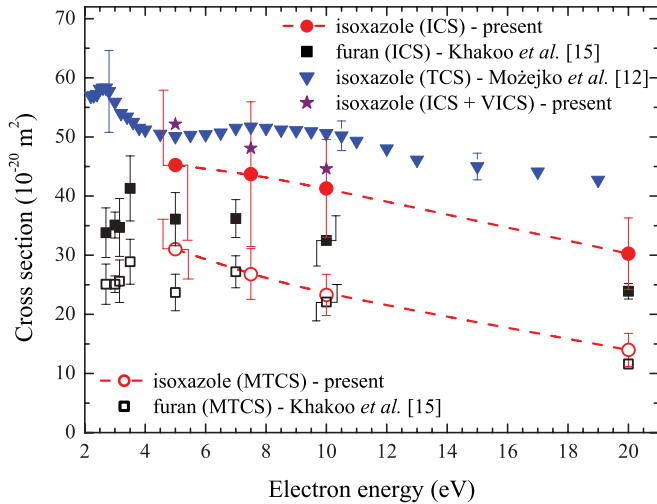
FIG. 4. (Color online) Elastic integral (ICS), momentum transfer (MTCS), and the sum of the elastic and vibrational integral (ICS + VICS) cross sections obtained in isoxazole. Also shown are the total cross section (TCS) measured in isoxazole by Możejko *et al.* [12] and the cross sections obtained in furan by Khakoo *et al.* [15].

transfer cross sections are reported in Fig. 4, where they are compared with the experimental cross sections of furan [15] and the total cross section of isoxazole [12]. They are also listed in Table II. The uncertainties in the integral cross section are estimated to be 28% at electron energies of 5 and 7.5 eV and 20% at 10 and 20 eV. The contributions from the adopted extrapolation procedure to the uncertainties are estimated as 20% and 10%, respectively, and are added in quadrature to the uncertainties of the integrated cross sections of 20% and 17%, respectively. The uncertainties in the momentum transfer cross section are 16% at electron energies 5–10 eV and 20% at 20 eV, where the contributions from the extrapolation are negligible (less than 0.5%).

The integral elastic cross section obtained in isoxazole (Fig. 4) decreases with the increase of the electron energy. At 5 eV, it exceeds that of furan [15], because of higher DCS in the whole angular range and at 7.5 and 10 eV due to higher DCSs for the forward scattering. The momentum transfer cross section of isoxazole coincides with that of furan [15] at 7.5 and 10 eV. Here, the contributions of the forward dipole scattering in both molecules are suppressed. At 5 eV, the isoxazole cross section has a higher value than that of furan, as a result of a higher DCS for the backward scattering.

B. Vibrational excitation

1. Energy-loss spectra

The energy-loss spectra in the region of vibrational excitation, measured at the incident electron energies of 5 and 10 eV, are reported in Figs. 5(a) and 5(b), respectively. The spectra display effective excitation of a number of vibrational fundamental modes, overtones, and combination modes of the isoxazole molecules. Some peaks in the energy-loss spectra, e.g., that at 0.113 eV in Fig. 5(a), show an increased width with respect to 50 meV (FWHM) of the elastic peak, which indicates overlapping of closely spaced vibrational peaks. To identify the vibrational modes excited, the energy-loss spectra were fitted with a number of Gaussian profiles, whose widths (FWHM) were set to be equal to that of the elastic peak. In the initial step of the fitting, to resolve the fundamental modes of vibrations the energy-loss spectra were fitted in the energy range up to 0.2 eV. In this range four energy-loss peaks gave excellent agreement with the overall shape of the spectra as it is shown in Figs. 5(a) and 5(b). However, it was also found that the best fits to the experimental curves were obtained for an increased width of 52 meV of the energy-loss peaks at 101 meV in both spectra. The increased widths indicate further contributions of at least two modes, whose vibrational energies differ by more than 5 meV, as shown by our computer simulations of the overlapping of two energy-loss peaks that have the same intensities. For the energy difference lower than 5 meV, a peak of essentially 50 meV width (FWHM) in the energy-loss spectrum will be produced. It is of note that although the relative intensities of the peaks are different in both spectra (Fig. 5), the energy positions of the corresponding peaks in the spectra were found to agree to within ±0.2 meV. The energies of the peaks resolved in the energy-loss spectra up to 0.2 eV are listed in Table III together with that corresponding to the C-H stretch vibrations, which are seen as single peaks of 50 meV width (FWHM). The energies of the peaks are compared in Table III with the vibrational frequences of the fundamental modes of isoxazole [29,30], which are most likely excited and observed as a single peak. In the next step of the fitting, the energy-loss spectra in the 0.2–0.65 eV range were examined. Here, the energy positions of the peaks due to the n overtone of the ν_i vibration and the ν_j plus ν_i combination vibrations were calculated within the harmonic approximation as $n\nu_i$ and $\nu_j + n\nu_i$, respectively. The intensities of these energy-loss peaks were found from fitting them to the measured spectra. In this scheme the positions of the 101-meV vibration overtones had to be slightly adjusted within ±2 meV. This approach gave an excellent agreement
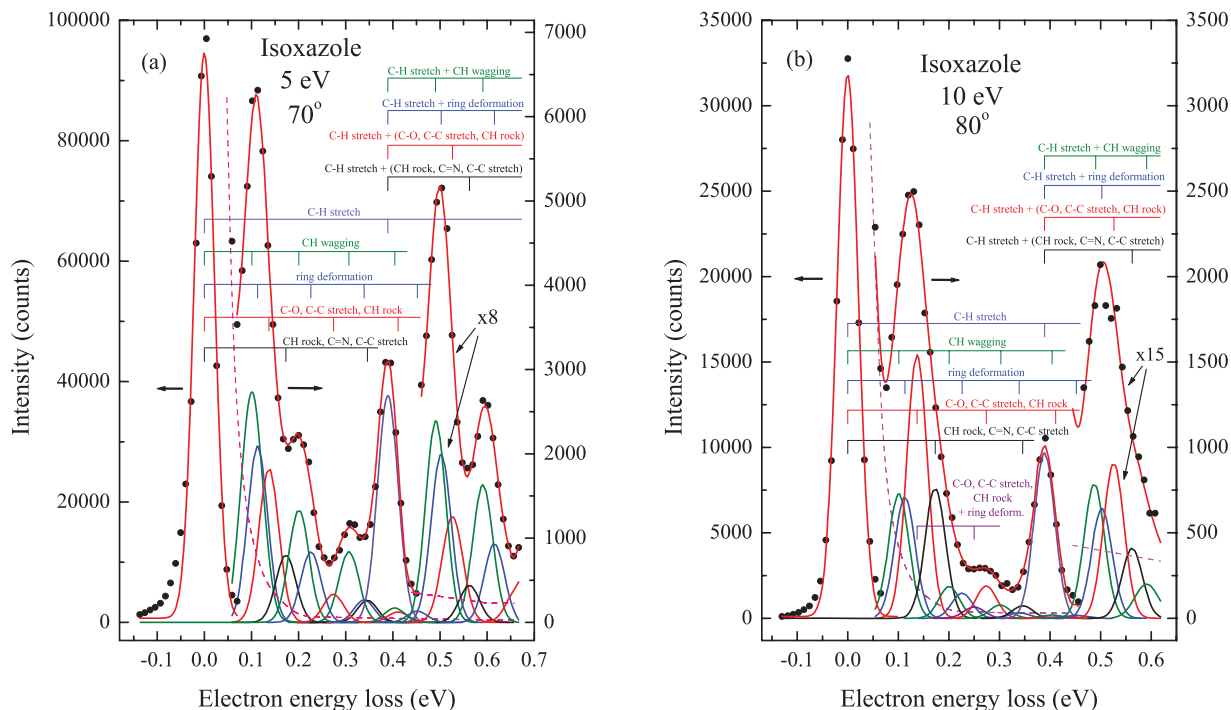
TABLE II. Integral elastic σ_{ie}, vibrational (C-H stretch) σ_{iv}, total σ_t, and momentum transfer σ_m cross sections, in units of 10^{-20} m², in isoxazole.

	Cross section			
	Elastic σ_{ie}	Vibrational (C-H stretch) σ_{iv}	Total[a] σ_t	Momentum transfer σ_m
5	45.3	1.19	50.1	31.0
7.5	43.7	0.803	51.7	26.8
10	41.3	0.557	50.6	23.3
20	30.3	–	42.2	14.0

[a]Reference [12].

FIG. 5. (Color online) Energy-loss spectra measured in isoxazole at the incident electron energy and scattering angle of (a) 5 eV and 70°, and (b) 10 eV and 80°. The excited vibrational modes fitted to the experimental curves and the final fits are shown by the solid lines. The energies of the fundamental, overtone, and combination vibrational modes are indicated by vertical bars. The dashed lines show the estimated background contributions.

with the measured energy-loss spectra in the whole energy range up to 0.65 eV, as it is shown in Figs. 5(a) and 5(b) by the final overal fits, supporting procedure used to resolve peaks of the fundamental modes. The contributions of the background and the tail of the elastic scattering in the energy-loss spectra were determined by flowing the target gas directly to the vacuum chamber. These contributions are indicated in Figs. 5(a) and 5(b) and were taken into account in the fitting.

The remarkable correlation between energies of the re-solved energy-loss peaks and the vibrational energies of the fundamental modes, which are on average within less than ± 3 meV of the centers of the peaks (Table III), demonstrates that at 5 and 10 eV the most likely excited vibrational modes of the isoxazole molecules are ν_{15}, ν_{13}: CH wagging and O-N stretch, respectively (peak at 101 meV); ν_{14}, ν_{12}, ν_{11}: CH wagging and ring deformation (113 meV); ν_9, ν_8: C-O stretch, C-C stretch, and CH rocking (137 meV); ν_6, ν_5: CH

TABLE III. Energies of the observed energy-loss peaks, details of the vibrational modes, and their description in isoxazole.

| Energy-loss peak (meV)	Vibrational mode	Symmetry	Vibrational energy (meV)[a]	Description[b]
101	ν_{15}	A''	98.2	CH wagging
	ν_{13}	A'	106.3	O-N stretch
113	ν_{14}	A''	110.3	CH wagging
	ν_{12}	A'	111.6	Ring deformation
	ν_{11}	A'	114.0	Ring deformation
137	ν_9	A'	135.9	C-O, C-C stretch
	ν_8	A'	140.1	CH rocking, C-O stretch
173	ν_6	A'	170.0	CH rocking, C-C stretch
	ν_5	A'	177.6	CH rocking, C-C, C = N stretch,
389	ν_2	A'	387.8	C-H stretch
	ν_1	A'	391.8	C-H stretch

[a]Reference [29].

[b]Reference [30].
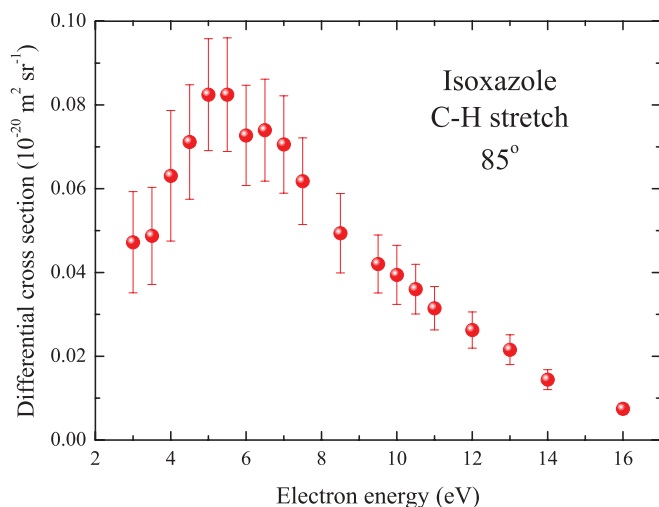
FIG. 6. (Color online) Differential cross section for excitation of the C-H stretch modes of isoxazole measured at a scattering angle of $85°$.
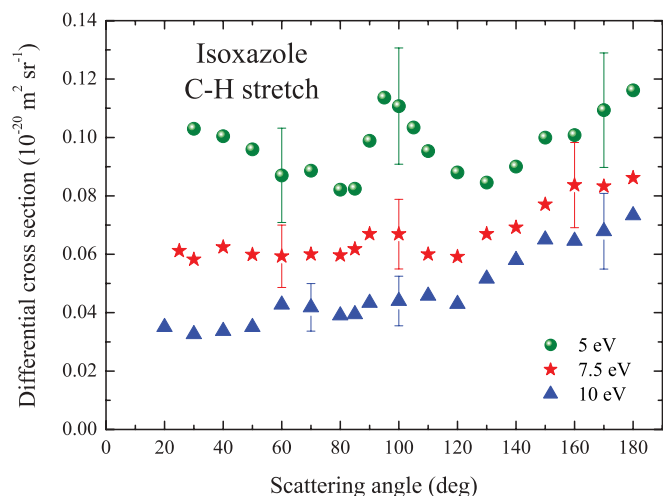

FIG. 7. (Color online) Differential cross sections for excitation of the C-H stretch modes of isoxazole measured at the incident electron energies of 5, 7.5, and 10 eV.

rocking, C-C stretch, and $C=N$ stretch (173 meV); and ν_2, ν_1: C-H stretch (389 meV). The series of the combination modes involve the C-H stretch modes plus the above individual modes and a weak series of ν_9, $\nu_8 + \nu_{14}$, ν_{12}, ν_{11} modes (at 10 eV only), as indicated in Figs. 5(a) and 5(b). The first overtone of the ν_2, ν_1 C-H stretch modes is seen at the energy loss of 776 meV (not shown in Fig. 5).

The strong excitation of the overtones and combination vibrational modes at 5 and 10 eV incident energy points at resonance excitation at these energies via temporary negative ion states of isoxazole. The relative intensities of the vibrational series discerned in the energy-loss spectra at 5- and 10-eV electron energies show differences. At 5 eV, the ν_{15}, ν_{13} series, the CH wagging and O-N stretch, respectively, is the most intense, while at 10 eV the highest intensity series is that of the ν_9, ν_8 modes, the C-O stretch, C-C stretch, and CH rocking. Moreover, the intensities of the overtones in the series decrease more rapidly with the increase of the excitation energy in the 10-eV spectrum. These differences suggest two resonance energy regions, near 5 and 10 eV, where the 10-eV resonance (or resonances) has a shorter lifetime (larger width).

2. Differential cross sections

To gain more insight into the resonance vibrational excitation, the DCS for excitation of the C-H stretch modes was measured. The energy dependence of the DCS obtained in the 3–16 eV energy range at a scattering angle of $85°$ is presented in Fig. 6. It shows a broad peak at 5.5 eV. Above the peak, from about 8.5 eV it decreases to a low value at 16 eV, displaying, however, a weak maximum at around 10 eV. This energy dependence points at two broad resonances at 5.5 and 10 eV. The recorded shape of the excitation cross section in isoxazole resembles closely that of the C-H stretch excitation of cyclopentane measured by Allan and Andric [31], further indicating that the resonance vibrational excitation is a feature of a number of the hydrocarbon molecules [31]. These resonances in cyclic hydrocarbons are assigned to σ^* shape resonances [31], which means that the incoming

electron is temporarily trapped at the σ^*-type orbital. The same assignment is applied to the observed isoxazole resonances. It is worth noting that measurements of the dissociative electron attachment spectra in isoxazole [32] showed a broad band in the 39 amu ($C_3H_3{}^-$) negative ions spectrum, extending from 5 to 13 eV with a maximum at 6.8 eV. These negative ions are presumably formed via the above resonances.

The angular dependences of the DCSs for the C-H stretch excitation were measured at 5, 7.5, and 10 eV in the $20°$–$180°$ range. These results are shown in Fig. 7 and their

TABLE IV. Differential cross sections, in units of 10^{-22} m^2 sr^{-1}, for excitation of the C-H stretch modes of the isoxazole molecules at the incident electron energies of 5, 7.5, and 10 eV. The absolute errors are shown in parentheses.

Scattering angle	Energy (eV)		
(degrees)	5	7.5	10
20	–	–	3.51 (1.02)
25	–	6.12 (2.26)	–
30	10.3 (3.0)	5.82 (1.45)	3.26 (0.95)
40	10.0 (2.3)	6.24 (1.12)	3.37 (0.77)
50	9.59 (2.21)	5.99 (1.08)	3.51 (0.67)
60	8.70 (1.57)	5.93 (1.07)	4.27 (0.81)
70	8.86 (1.59)	6.00 (1.08)	4.18 (0.79)
80	8.21 (1.48)	5.97 (1.07)	3.91 (0.74)
85	8.25 (1.48)	6.18 (1.11)	3.94 (0.75)
90	9.89 (1.78)	6.69 (1.20)	4.33 (0.82)
95	11.4 (2.05)	–	–
100	11.1 (2.0)	6.69 (1.20)	4.40 (0.83)
105	10.3 (1.9)	–	–
110	9.53 (1.72)	6.00 (1.08)	4.58 (0.87)
120	8.80 (1.58)	5.91 (1.06)	4.30 (0.82)
130	8.46 (1.52)	6.69 (1.20)	5.16 (0.98)
140	9.00 (1.62)	6.92 (1.24)	5.80 (1.10)
150	9.99 (1.80)	7.71 (1.39)	6.50 (1.23)
160	10.1 (1.8)	8.37 (1.51)	6.46 (1.23)
170	10.9 (2.0)	8.33 (1.50)	6.79 (1.29)
180	11.6 (2.1)	8.61 (1.55)	7.33 (1.39)

numerical values are displayed in Table IV together with the estimated uncertainties. The 5- and 10-eV dependences differ substantially. The 5-eV curve shows a rather sharp rise to a maximum at about 95°–100° and increases at low and high scattering angles. This shape of the angular distribution suggests a higher partial wave in the scattering, presumably that of $l = 2$, $m = 2$. However, as seen from the fitting in Fig. 5(a), the measured C-H stretch excitation signal may include excitation of the $4\nu_{15}$, $4\nu_{13}$ and $3\nu_9$, $3\nu_8$ overtones. This contribution is estimated at about 10%. The angular distribution at 10 eV is nearly isotropic up to 120° but shows an increase at higher scattering angles. This angular behavior may suggest the contribution of several partial waves and also of some direct scattering. The 7.5-eV curve is a superposition of both above angular distributions as a result of overlapping of the resonances. The DCSs were integrated over the 0°–180° angular range, after extrapolation down to 0° scattering angle, to yield the integral cross sections for the C-H stretch excitation. They are included in Table II.

IV. CONCLUSIONS

The DCSs for elastic electron scattering in isoxazole were measured at the energies of 5, 7.5, 10, and 20 eV over the scattering angle range from 10° to 180°. These results were compared with the DCSs obtained in furan [15], which is isoelectronic to isoxazole. However, both molecules differ quite substantially in the value of their dipole moments. It was found that in the 5–10 eV energy range, the DCSs for the forward scattering in isoxazole (below 60°) show a steeper increase with the decreasing scattering angle than that in furan, validating its higher electric dipole moment. On the other hand, in the 60°–180° angular range, the DCSs of both molecules in the 7.5–20 eV range coincide to a high degree.

The elastic DCS measured in the 2–20 eV range in isoxazole at a scattering angle of 85° reveals a π^* (π_5^*) resonance at 2.7 eV, which corresponds to that at 3.10 eV in furan [15].

The elastic integral and momentum transfer cross sections were deduced in isoxazole at 5, 7.5, 10, and 20 eV from the DCSs measured over a wide scattering angle range, applying extrapolation of the DCSs in a short range below 30°. These cross sections were compared with those determined in furan [15].

The excitation of overtones and combination vibrational modes of isoxazole molecules identified in the energy-loss spectra measured at 5 and 10 eV points at resonance excitation via the temporary negative ion states of isoxazole. The ring deformation accompanied by the ring bonds stretching and the C-H vibrations are the modes excited with the highest intensities. The C-H stretching modes are excited via the shape resonances at 5.5 and 10 eV, most likely the σ^* resonances, which show different angular distributions in the electron scattering.

The DCS for excitation of the C-H stretch modes was determined at 5, 7.5, and 10 eV over the 20°–180° angular range, and after extrapolation to 0° was integrated to obtain the integral C-H stretch cross section. The vibrational integral cross section (sum of all vibrational modes) was estimated using the C-H stretch excitation cross section and the measured energy-loss spectra to be (6.9, 4.4, and 3.3) × 10^{-20} m^2 at 5, 7.5, and 10 eV, respectively. The sum of the vibrational integral cross section and the elastic integral cross section is compared in Fig. 4 with the total cross section of Ref. [12]. At 5 eV, where the electronic excitation and dissociative electron attachment are very weak, the sum of the integral elastic and vibrational cross sections of 52.2 × 10^{-20} m^2 agrees reasonably well, taking into account a simple estimation of the vibrational cross section, with the total cross section of 50.1 × 10^{-20} m^2.

Finally, it is hoped that the results of this study will stimulate theoretical works on electron collisions with the isoxazole molecules.

[1] B. Boudaïffa, P. Cloutier, D. Hunting, M. A. Huels, and L. Sanche, Science **287**, 1658 (2000).

[2] M. A. Huels, B. Boudaïffa, P. Cloutier, D. Hunting, and L. Sanche, J. Am. Chem. Soc. **125**, 4467 (2003).

[3] M. Fuss, A. Munoz, J. C. Oller, F. Blanco, P. Limão-Vieira, C. Huerga, M. Tellez, M. J. Hubin-Fraskin, K. Nixon, M. Brunger, and G. Garcia, J. Phys.: Conf. Ser. **194**, 012028 (2009).

[4] D. N. Slatkin, P. Spanne, F. A. Dilmanian, and M. Sandborg, Med. Phys. **19**, 1395 (1992).

[5] A. Gemmel, B. Hasch, M. Ellerbrock, W. K. Weyrather, and M. Krämer, Phys. Med. Biol. **53**, 6991 (2008).

[6] I. Linert, B. Mielewska, G. C. King, and M. Zubek, Phys. Rev. A **81**, 012706 (2010).

[7] A. Modelli and P. D. Burrow, J. Phys. Chem. A **108**, 5721 (2004).

[8] P. Pevarello, R. Amici, M. G. Brasca, M. Villa, and M. Varasi, Targets Heterocycl. Syst. **3**, 301 (1999).

[9] *CRC Handbook of Chemistry and Physics*, 85th ed., edited by D. R. Lide (CRC Press, Boca Raton, FL, 2004–2005).

[10] K. Jug, S. Chiodo, P. Calaminici, A. Avramopoulos, and M. G. Papadopoulos, J. Phys. Chem. A **107**, 4172 (2003).

[11] I. C. Walker, M. H. Palmer, J. Delwiche, S. V. Hoffmann, P. Limão-Vieira, N. J. Mason, M. F. Guest, M.-J. Hubin-Franskin, J. Heinesch, and A. Giuliani, Chem. Phys. **297**, 289 (2004).

[12] P. Możejko, E. Ptasińska-Denga, and Cz. Szmytkowski, Eur. Phys. J. D **66**, 44 (2012).

[13] I. Linert, I. Lachowicz, T. J. Wasowicz, and M. Zubek, Chem. Phys. Lett. **498**, 27 (2010).

[14] G. Bouchoux and Y. Hoppilliard, Org. Mass Spectrom. **16**, 459 (1981).

[15] M. A. Khakoo, J. Muse, K. Ralphs, R. F. da Costa, M. H. F. Bettega, and M. A. P. Lima, Phys. Rev. A **81**, 062716 (2010).

[16] F. Motte-Tollet, G. Eustatiu, and D. Roy, J. Chem. Phys. **105**, 7448 (1996).

[17] L. R. Hargreaves, R. Albaridy, G. Serna, M. C. A. Lopes, and M. A. Khakoo, Phys. Rev. A **84**, 062705 (2011).

[18] C. Szmytkowski, P. Możejko, E. Ptasińska-Denga, and A. Sabisz, Phys. Rev. A **82**, 032701 (2010).

[19] I. Linert and M. Zubek, J. Phys. B **39**, 4087 (2006).

[20] F. H. Read and J. M. Channing, Rev. Sci. Instrum. **67**, 2372 (1996).

[21] J. C. Gibson, R. J. Gulley, J. P. Sullivan, S. J. Buckman, V. Chan, and P. D. Burrow, J. Phys. B: At. Mol. Opt. Phys. **29**, 3177 (1996).

[22] K. Franz, T. H. Hoffmann, J. Bömmels, A. Gopalan, G. Sauter, W. Meyer, M. Allan, M. W. Ruf, and H. Hotop, Phys. Rev. A **78**, 012712 (2008).

[23] J. C. Nickel, C. Mott, I. Kanik, and D. C. McCollum, J. Phys. B **21**, 1867 (1988).

[24] R. K. Nesbet, Phys. Rev. A **20**, 58 (1979).

[25] H. P. Saha, Phys. Rev. A **40**, 2976 (1989).

[26] *Landolt-Börnstein, Zahlenwerte und Funktionen, Bd I, Atom und Molekularphysik, 1, Atome und Ionen*, edited by A. Eucken (Springer-Verlag, Berlin, 1950).

[27] M. Allan, J. Phys. B **40**, 3531 (2007).

[28] M. H. F. Bettega and M. A. P. Lima, J. Chem. Phys. **126**, 194317 (2007).

[29] E. G. Robertson, J. Mol. Spectrosc. **231**, 50 (2005).

[30] A. El-Azhary and H. U. Suter, J. Phys. Chem. **99**, 12751 (1995).

[31] M. Allan and L. Andric, J. Chem. Phys. **105**, 3559 (1996).

[32] M. Dampc and M. Zubek, 2012 (unpublished).